

Supplementary Materials

Supramolecular Self-Assembled Nanostructures Derived from Amplified Structural Isomerism of Zn(II)–Sn(IV)–Zn(II) Porphyrin Triads and Their Visible Light Photocatalytic Degradation of Pollutants

Nirmal Kumar Shee and Hee-Joon Kim*

Department of Chemistry and Bioscience, Kumoh National Institute of Technology

61 Daehak-ro, Gumi 39177, Republic of Korea

List of contents:

Figure S1. ^1H NMR spectrum of 5,10-bis(3-pyridyl)-15,20-bis(phenyl)porphyrin **H₂P** in CDCl_3 .

Figure S2. ^1H NMR spectrum of *trans*-dihydroxo-[5,10-bis(3-pyridyl)-15,20-bis(phenyl)porphyrinato]tin(IV) **SnP¹** in CDCl_3 .

Figure S3. ^1H NMR spectrum of **T1** in DMSO-d_6 .

Figure S4. ESI-mass spectrum of **T1**.

Figure S5. Adsorption and desorption isotherms of N_2 for **T1** and **T2** at 77 K.

Figure S6. RhB dye adsorption test of **T1** and **T2**.

Figure S7. Absorption spectra of RhB in the presence of **T2** under visible light irradiation.

Figure S8. Kinetics of the photocatalytic degradation of RhB under visible light irradiation.

Figure S9. Absorption spectra of TC in the presence of **T2** under visible light irradiation.

Figure S10. Kinetics of the photocatalytic degradation of TC under visible light irradiation.

Figure S11. Recyclability of the photocatalyst **T2** towards the degradation of RhB.

Figure S12. FE-SEM images of **T1** and **T2** (after and before the degradation of RhB).

Figure S13. FT-IR spectra **T1** (after and before the degradation of RhB).

Figure S14. PXRD spectra **T1** (after and before the degradation of RhB).

Figure S15. Effect of temperature on the photocatalytic degradation of RhB in the presence of **T2**.

Figure S16. Effect of pH on the degradation of RhB solution in the presence of **T2**.

Figure S17. Effect of dye concentration on the photocatalytic degradation of RhB in the presence of **T2**.

Figure S18. Effect of wavelength dependence on the photocatalytic degradation of RhB in the presence of **T2**.

Figure S19. Positive ion mode ESI-mass spectrum of the RhB degradation reaction by **T2** after 45 min of visible light irradiation.

Figure S20. Band gap energy of **T1** and **T2** calculated from the Tauc's plot using absorption spectral data.

Figure S21. Photocurrent responses for **T1** and **T2** under visible light.

Figure S22. EIS Nyquist plots for **T1** and **T2** under visible light.

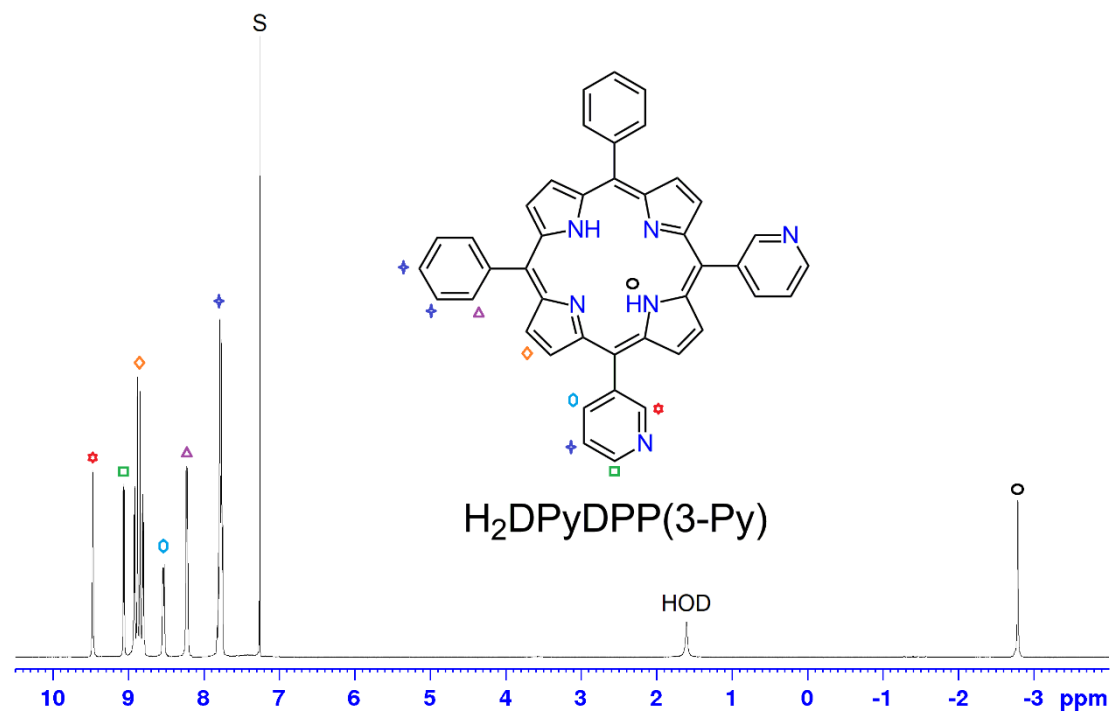


Figure S1. ¹H NMR spectrum of 5,10-bis(3-pyridyl)-15,20-bis(phenyl)porphyrin **H₂P** in CDCl₃.

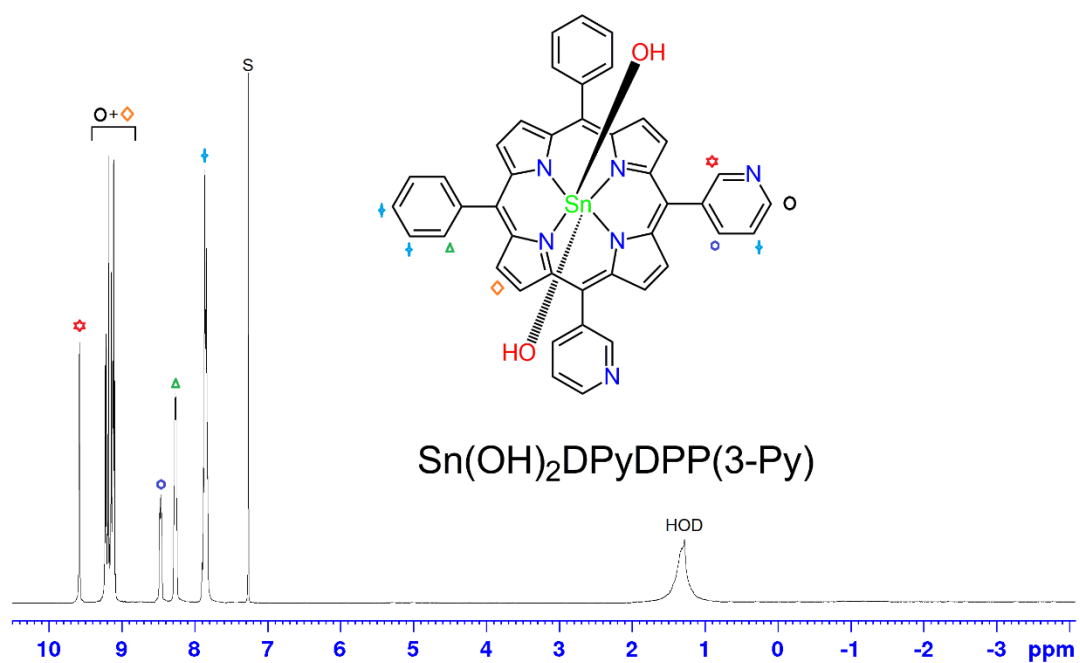


Figure S2. ¹H NMR spectrum of *trans*-dihydroxo-[5,10-bis(3-pyridyl)-15,20-bis(phenyl)porphyrinato]tin(IV) **SnP¹** in CDCl₃.

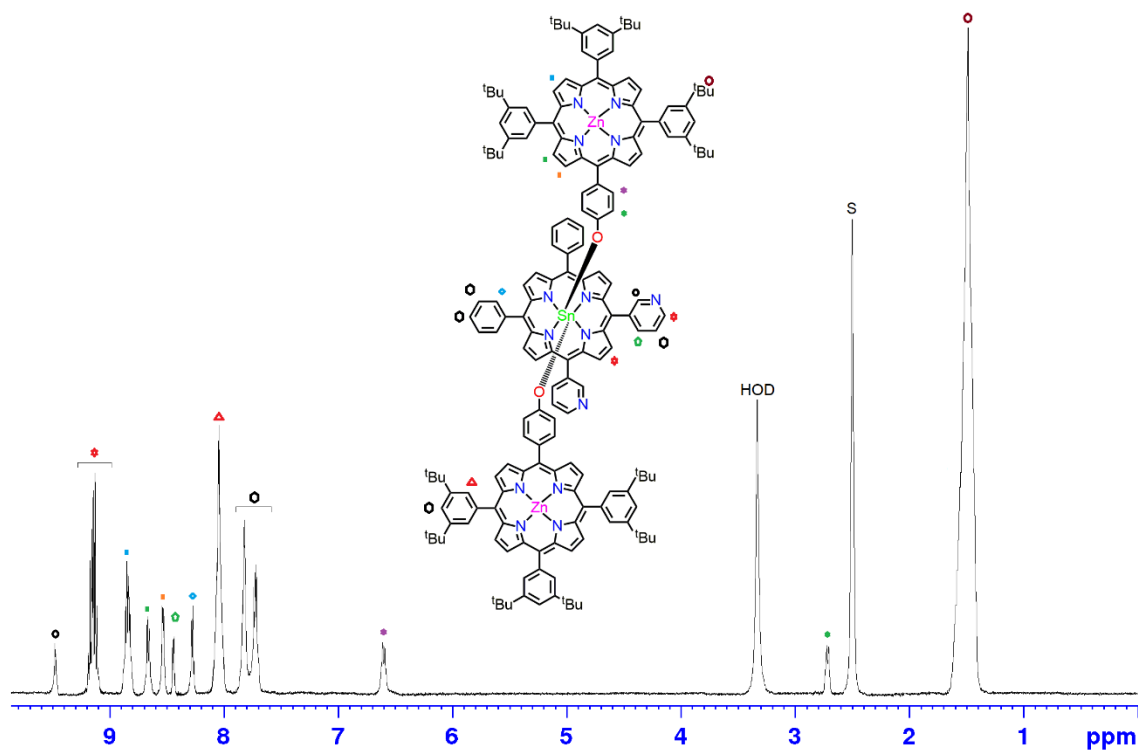


Figure S3. ^1H NMR spectrum of T1 in DMSO-d_6 .

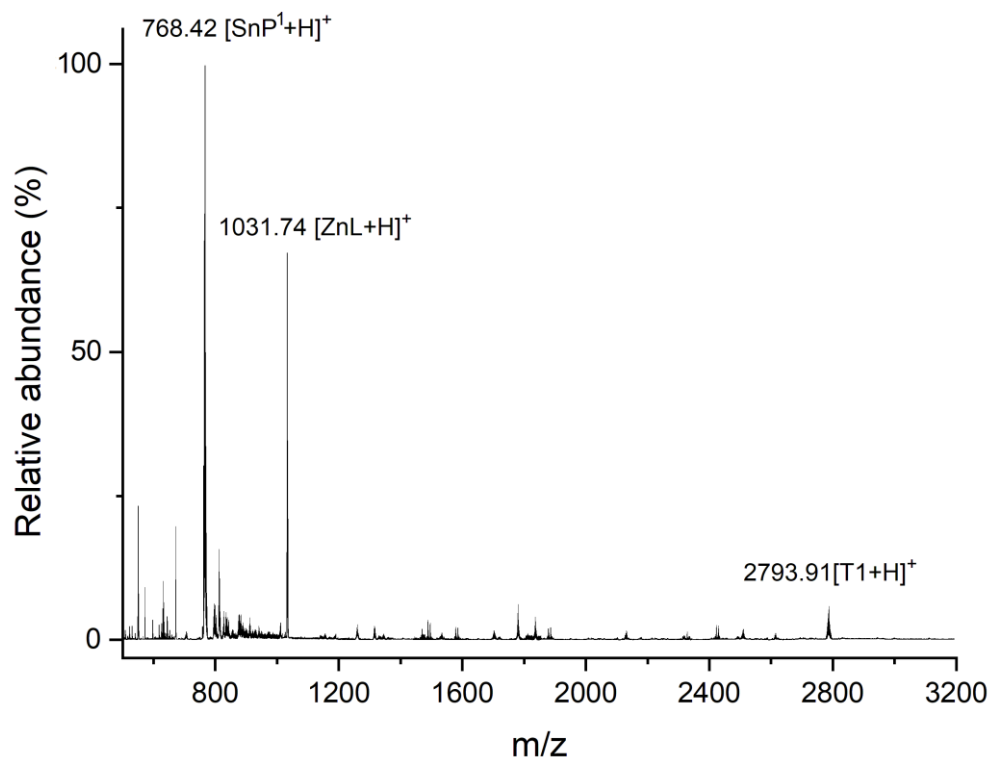


Figure S4. ESI-mass spectrum of T1.

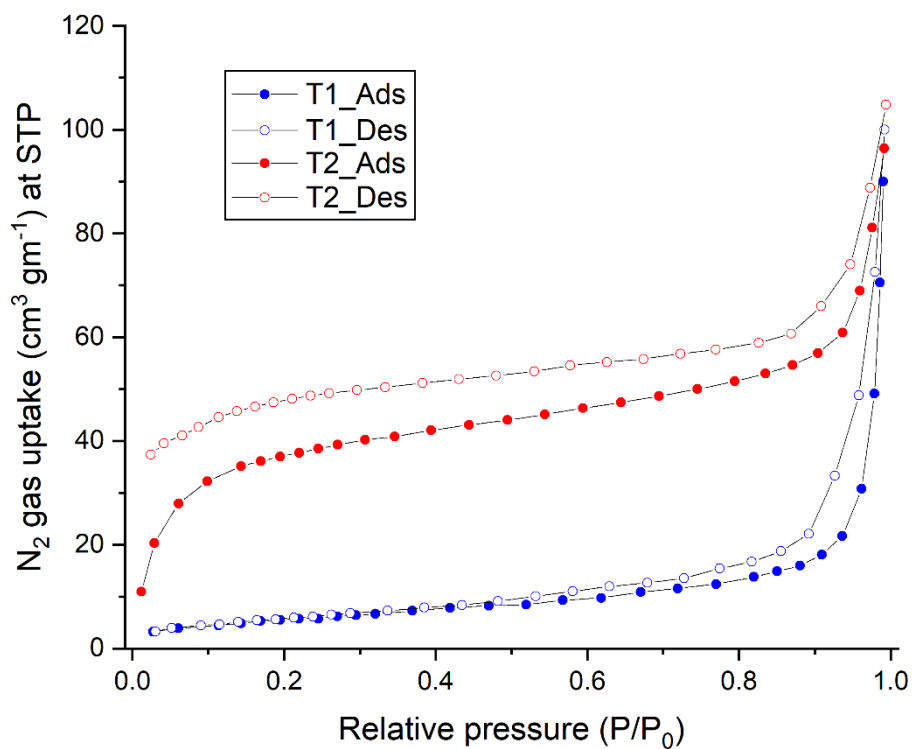


Figure S5. Adsorption and desorption isotherms of N₂ for T1 and T2 at 77 K.

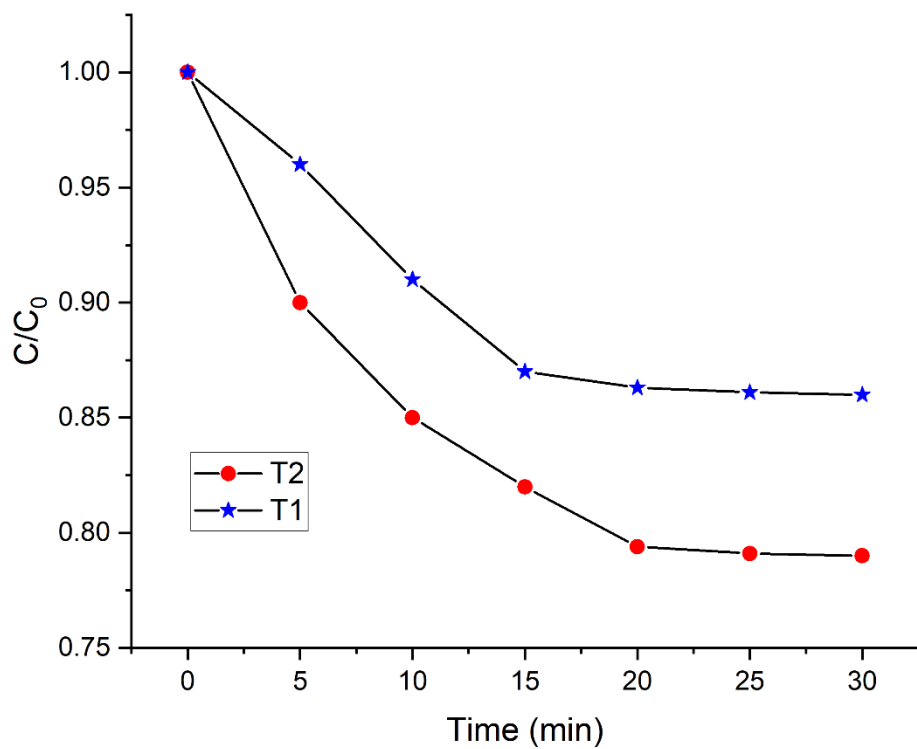


Figure S6. RhB dye adsorption test of T1 and T2.

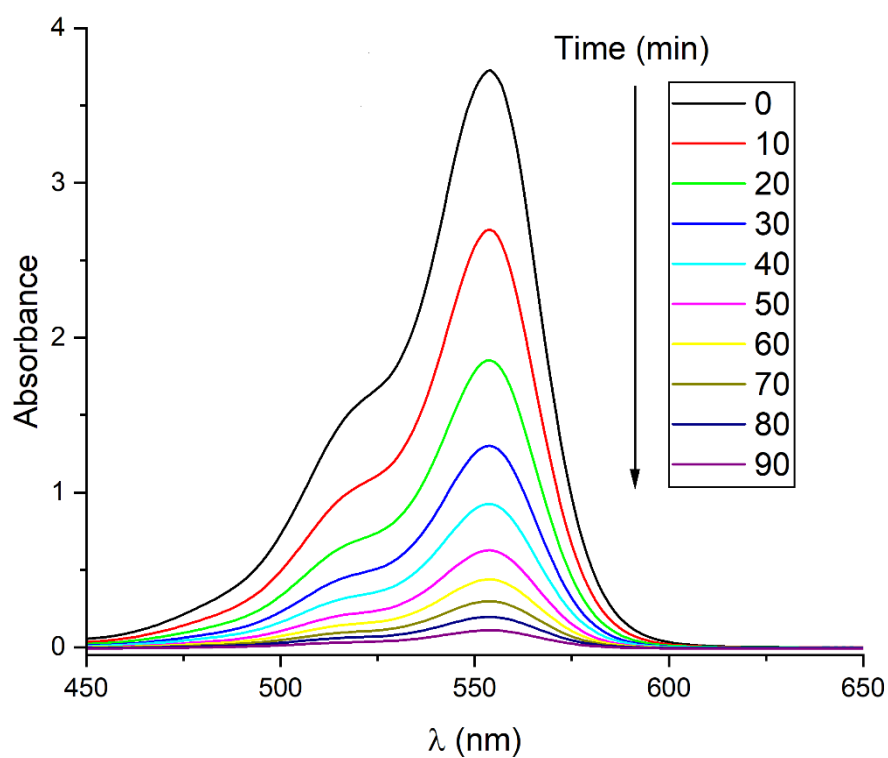


Figure S7. Absorption spectra of RhB in the presence of T2 under visible light irradiation.

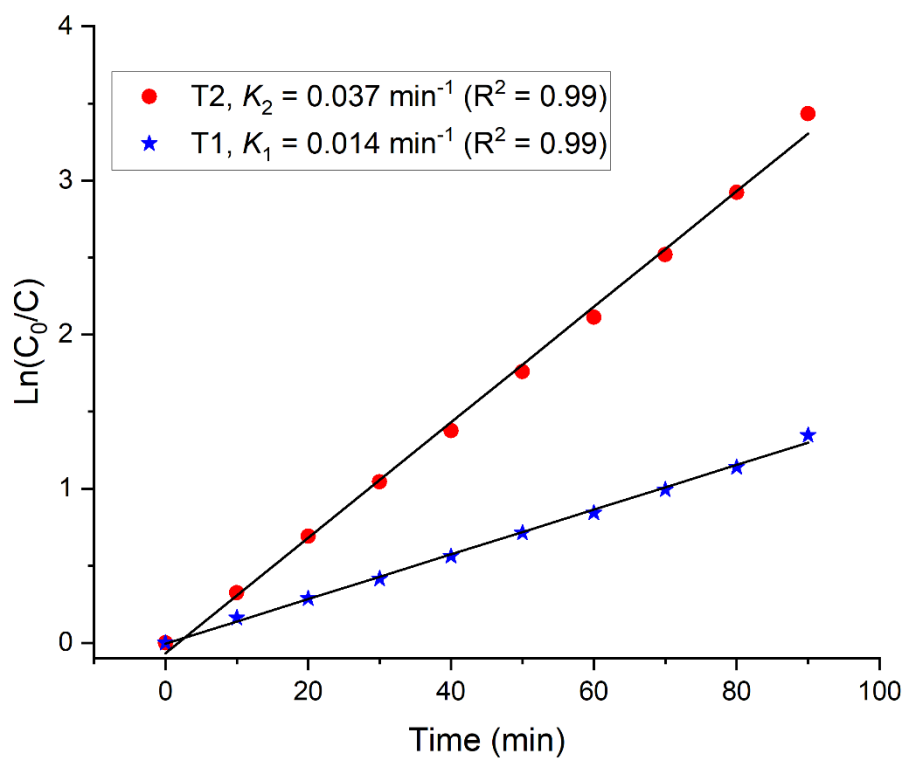


Figure S8. Kinetics of the photocatalytic degradation of RhB under visible light irradiation.

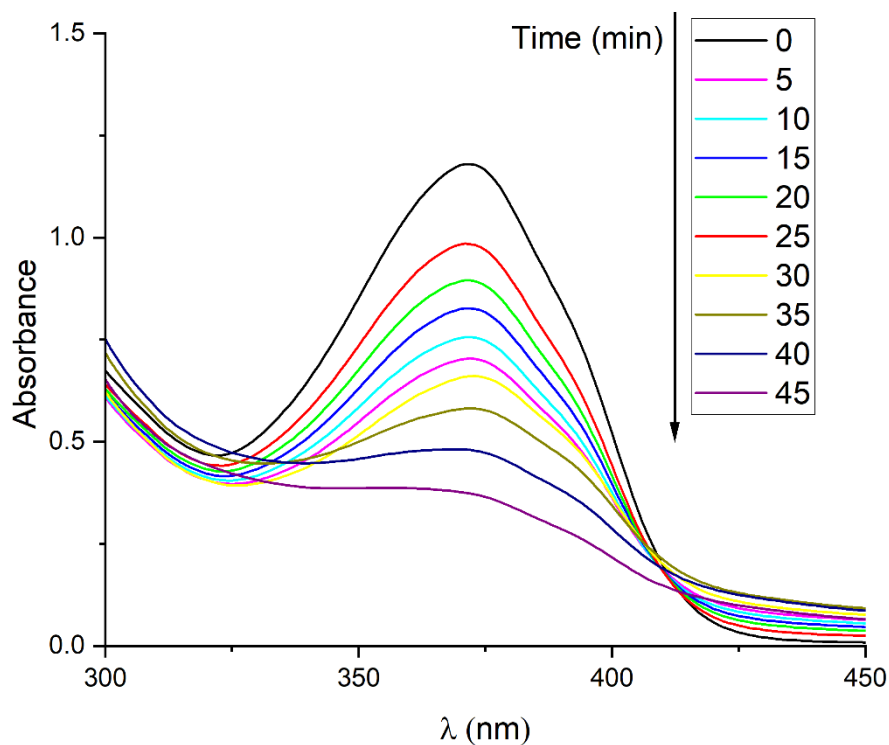


Figure S9. Absorption spectra of TC in the presence of T2 under visible light irradiation.

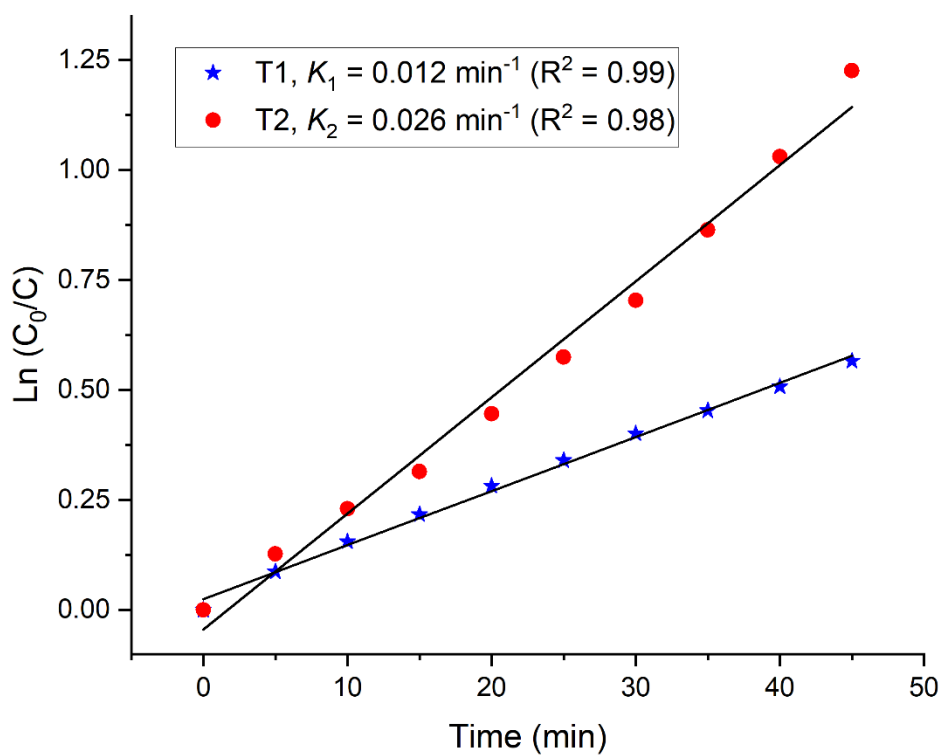


Figure S10. Kinetics of the photocatalytic degradation of TC under visible light irradiation.

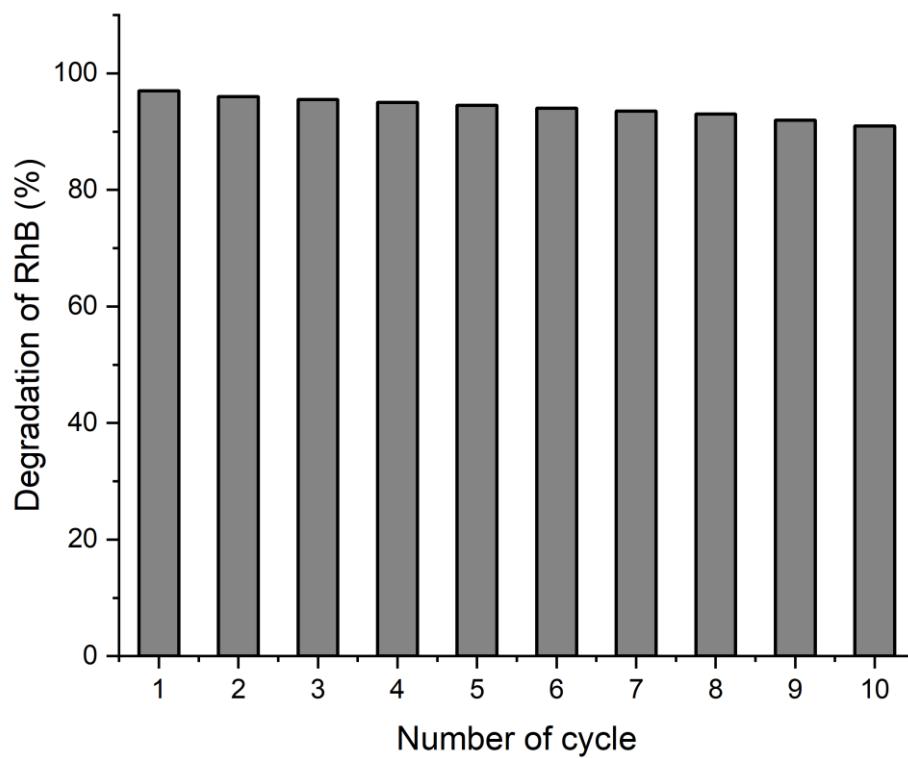


Figure S11. Recyclability of the photocatalyst **T2** towards the degradation of RhB.

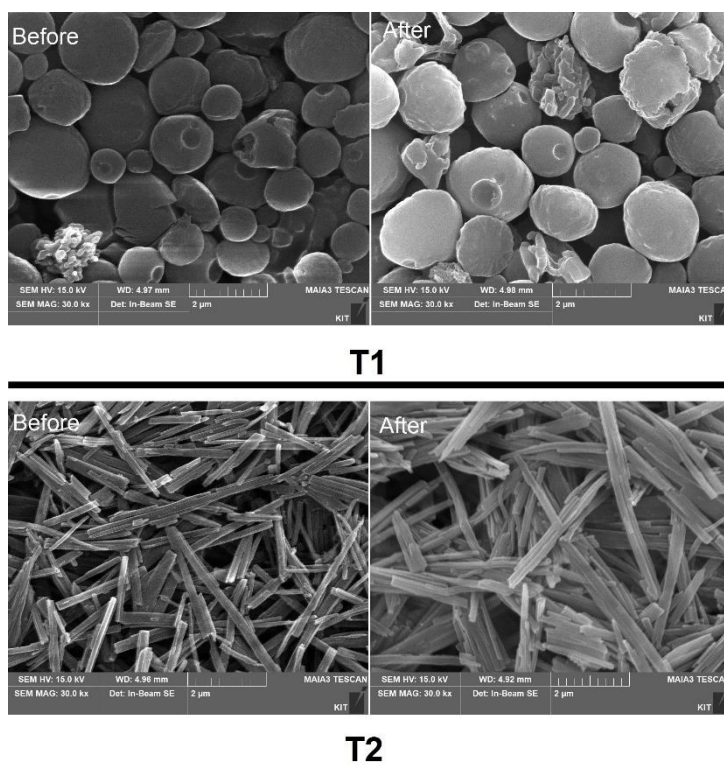


Figure S12. FE-SEM images of **T1** and **T2** (after and before the degradation of RhB).

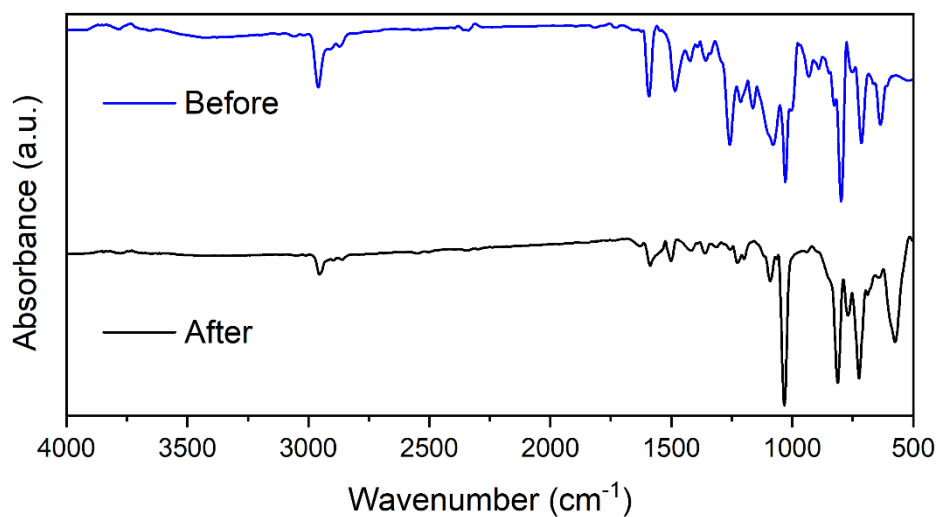


Figure S13. FT-IR spectra T1 (after and before the degradation of RhB).

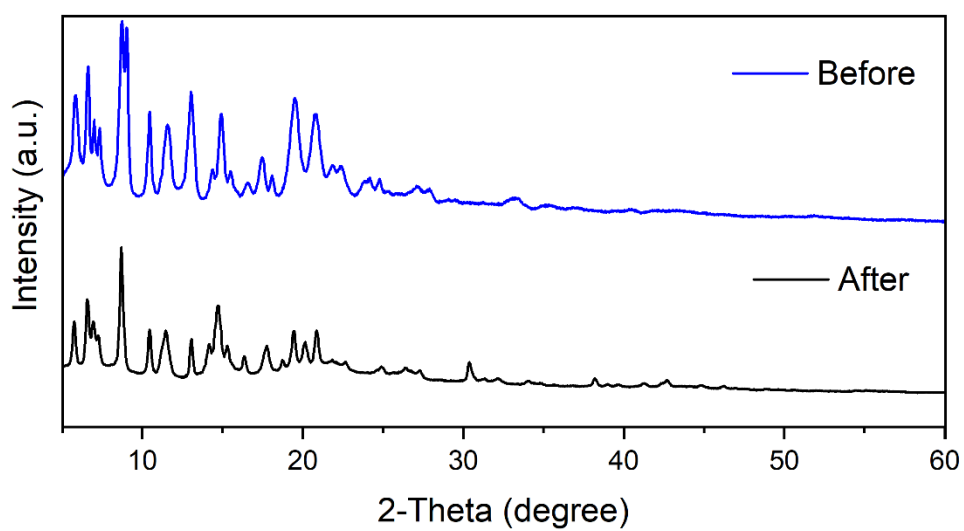


Figure S14. PXRD spectra T1 (after and before the degradation of RhB).

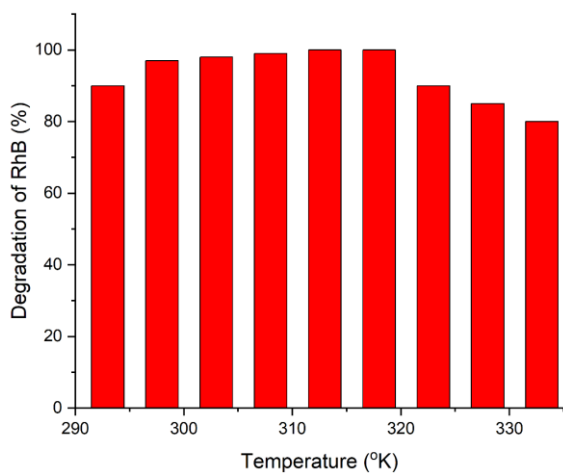


Figure S15. Effect of temperature on the photocatalytic degradation of RhB in the presence of T2.

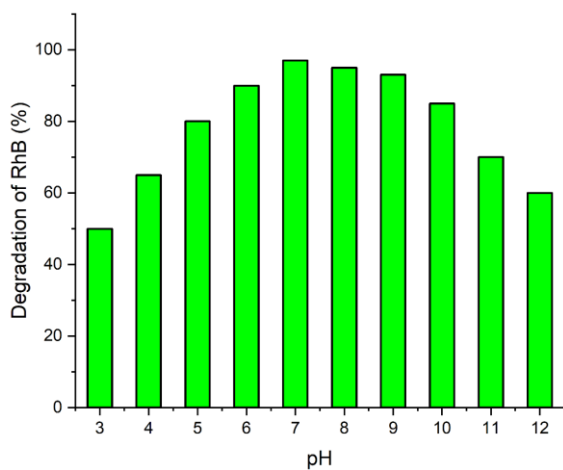


Figure S16. Effect of pH on the degradation of RhB solution in the presence of T2.

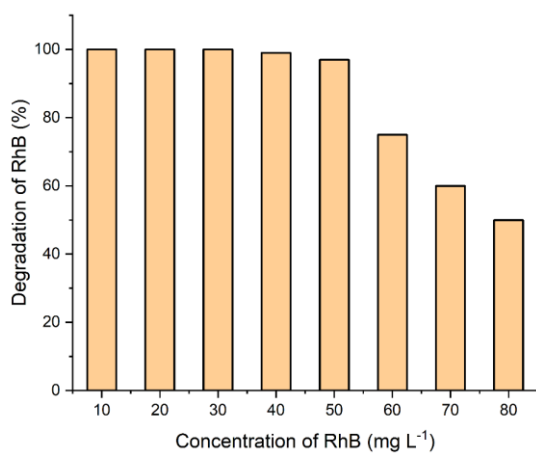


Figure S17. Effect of dye concentration on the photocatalytic degradation of RhB in the presence of T2.

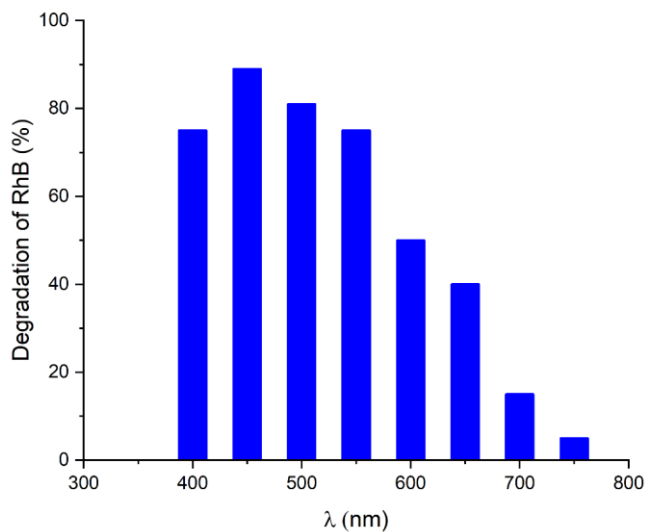


Figure S18. Effect of wavelength dependence on the photocatalytic degradation of RhB in the presence of T2.

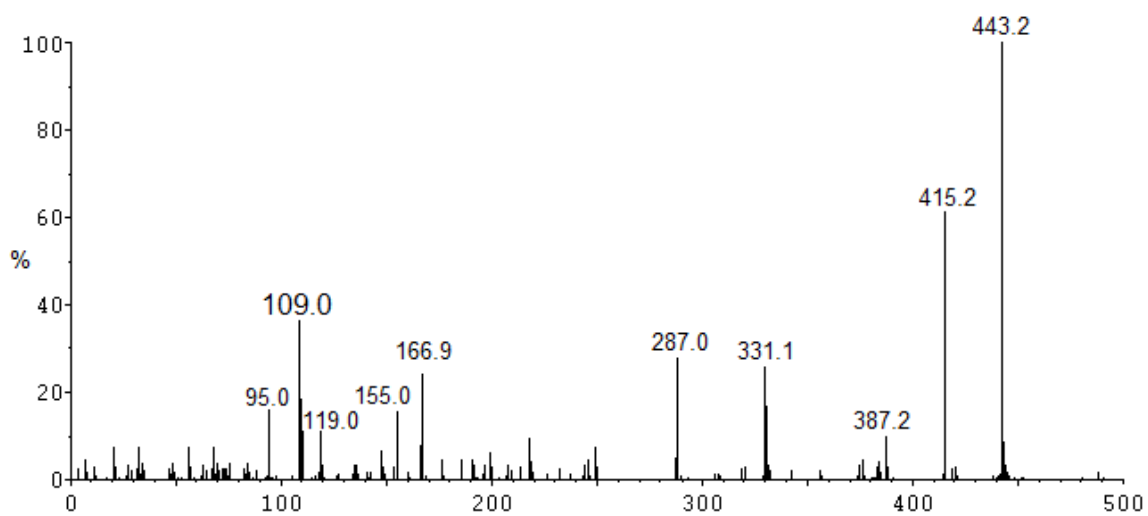


Figure S19. Positive ion mode ESI-mass spectrum of the RhB degradation reaction by T2 after 45 min of visible light irradiation.

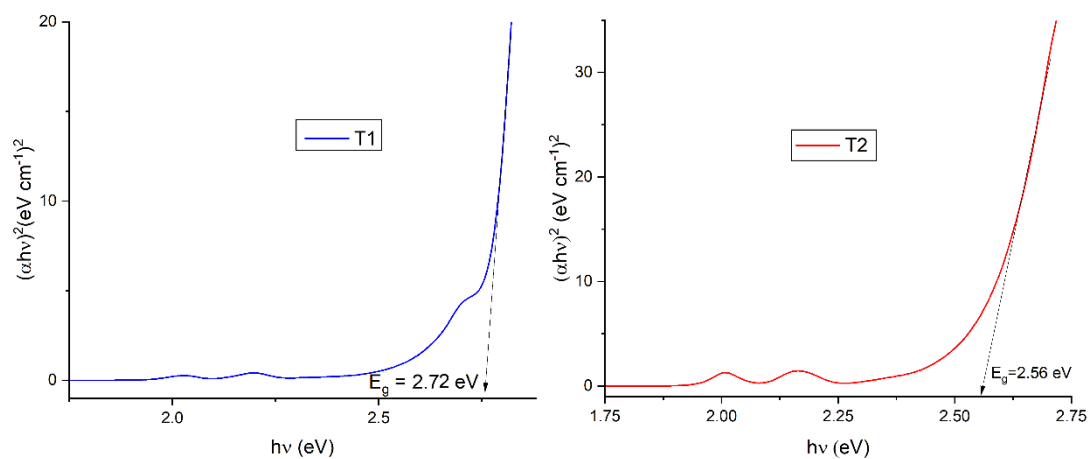


Figure S20. Band gap energy of T1 and T2 calculated from the Tauc's plot using absorption spectral data.

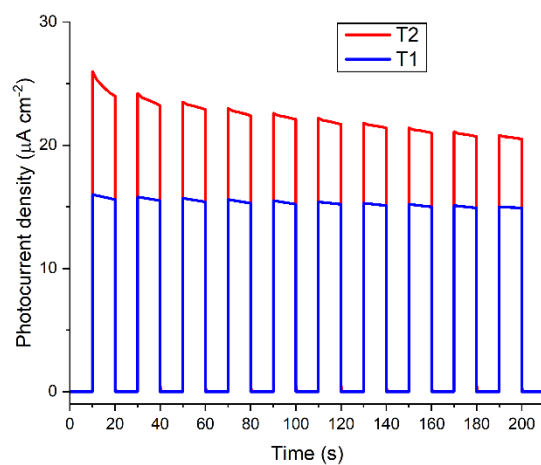


Figure S21. Photocurrent responses for T1 and T2 under visible light.

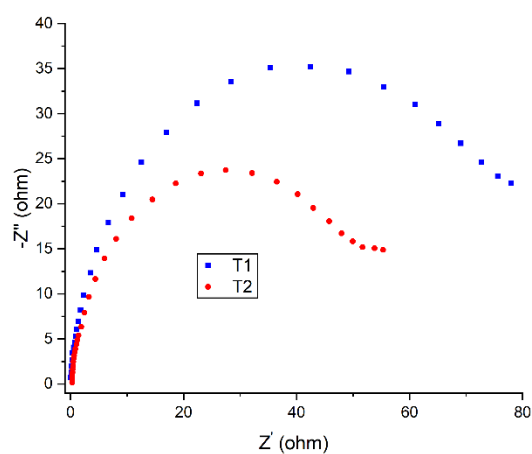


Figure S22. EIS Nyquist plots for T1 and T2 under visible light.